

LA-UR- 01-2521

Approved for public release;
distribution is unlimited.

Title: THERMAL SHOCK BEHAVIOR OF ALUMINA/MoSi₂
PLASMA SPRAYED LAMINATED COMPOSITES

Author(s): Daniel Mendoza, MST-6
Richard G. Castro, MST-6
John J. Petrovic, MST-8
Rajendra Vaidya, NMT-16

Submitted to: 3rd International Symposium on Applied Plasma Science
Conference held in Fairbank, Alaska on July 2-6, 2001



3 9338 00748 8256

Los Alamos

NATIONAL LABORATORY

Los Alamos National Laboratory, an affirmative action/equal opportunity employer, is operated by the University of California for the U.S. Department of Energy under contract W-7405-ENG-36. By acceptance of this article, the publisher recognizes that the U.S. Government retains a nonexclusive, royalty-free license to publish or reproduce the published form of this contribution, or to allow others to do so, for U.S. Government purposes. Los Alamos National Laboratory requests that the publisher identify this article as work performed under the auspices of the U.S. Department of Energy. Los Alamos National Laboratory strongly supports academic freedom and a researcher's right to publish; as an institution, however, the Laboratory does not endorse the viewpoint of a publication or guarantee its technical correctness.

Thermal Shock Behavior of Alumina/Molybdenum Disilicide Plasma Sprayed Laminated Composites

Daniel Mendoza, Richard Castro, John Petrovic, Raj Vaidya*

Los Alamos National Laboratory, Materials Science & Technology Division

*Los Alamos National Laboratory, Nuclear Materials Technology Division
Los Alamos, NM 87545

ABSTRACT

Alumina (Al_2O_3) is very susceptible to thermal shock, which leads to strength degradation. By reinforcing Al_2O_3 with molybdenum disilicide ($MoSi_2$) layers, the tolerance to damage caused by thermal shock can be improved. The thermal shock resistance of plasma sprayed $Al_2O_3/MoSi_2$ laminated composites were investigated. Three laminate microstructures having different layer thickness were fabricated by atmospheric plasma spraying while maintaining a 50/50-volume fraction. Quenching experiments done on 4-point bend bars showed a gradual decrease in the strength as the change in temperature (ΔT) increased. Thermal shock resistant parameters (R' and R'''') provided a representative numerical value of the thermal shock resistance for the laminated composites. The corresponding material properties for the different microstructures were determined experimentally in order to calculate the R' and R'''' values. The intermediate layered composite showed the highest R'''' value at $1061 \mu m$, while the thin layered composite had the highest R' value at $474 W/m$.

Key words: atmospheric plasma spraying, thermal shock resistance, composites, alumina, molybdenum disilicide

1. INTRODUCTION

The thermal shock behavior of brittle materials, such as ceramics, is a very critical parameter in evaluating the performance of the material for high temperature applications. When these materials are subjected to severe thermal gradient changes, cracking and damage will occur due to the thermal stresses [1]. Degradation in the strength can be seen, along with decreases in other important material properties; such as modulus and thermal conductivity. Studies investigating the thermal shock behavior of materials originated from theoretical work based on the thermoelastic theory [2]. Experimental studies involving the thermal shock behavior of materials have been investigated by several authors [3-14].

Evaluation of the thermal shock resistance of materials is typically done through various forms of rapid cooling methods that result in a destructive test in order to determine the change in the material property. However, numerical calculations of the thermal shock resistance of materials can also be determined from relationships derived from thermal stress conditions. Numerous thermal shock resistant relationships have been derived and are available, two principle approaches are

used to select and design materials. One approach looks at the avoidance of fracture initiation (R'), while the other looks at the avoidance of catastrophic crack propagation (R''''):

$$R' = \frac{k\sigma_f(1-\nu)}{E\alpha} \quad (1)$$

$$R'''' = \frac{K_{IC}^2}{\sigma_f^2(1-\nu)} \quad (2)$$

where E is the Young's modulus, σ_f is the fracture strength, ν is Poisson's ratio, α is the CTE, K_{IC} is fracture toughness, and k is the thermal conductivity. For the fracture initiation criteria (R'), fracture will occur when the thermal stresses reach the fracture stress of the material. The favorable material characteristics for avoiding fracture initiation by thermal shock are high values of strength and thermal conductivity coupled with low values of modulus and coefficient of thermal expansion. However, fracture may be avoided in certain materials through energy absorbing mechanisms such as crack deflection and bridging which are caused by pores, grain boundaries, and second phase materials. These considerations lead to the second criteria of crack propagation, which the driving force is associated with the stored elastic energy available in the material. A noncatastrophic fracture can occur when the total elastic energy is less than the total fracture energy required to propagate a crack [3,15]. The favorable material characteristics for minimizing the extent of crack propagation are high values of modulus and fracture toughness coupled with a low value of strength.

Conventionally processed Al_2O_3 shows a thermal shock threshold at 200-300°C, which makes processing ceramics for thermal shock resistant applications crucial. Plasma sprayed materials have been reported to have excellent thermal shock resistance due to their unique layered splat microstructure. Plasma spraying process also offers numerous advantages such as flexibility to manufacture continuous and discontinuous composites, solidification and consolidation all in one step, ability to tailor properties, and the capability for near-net shape products [16-19].

The purpose of this research is to improve the thermal shock behavior of Al_2O_3 by plasma spraying laminated composites with molybdenum disilicide ($MoSi_2$) and evaluating R' and R'''' to experimental data.

2. EXPERIMENTAL PROCEDURE

Atmospheric plasma sprayed materials, using a Praxair Surface Technology SG100 plasma torch, were used in this investigation. A dual powder feeding arrangement was used to deposit the alternating layers of Al_2O_3 and $MoSi_2$ into a tube geometry, Figure 1. The operating parameters for the plasma sprayed tubes are given in Table 1. The Al_2O_3 powder (Metco 105NS) had an average particle size of 45 μm and consisted of approximately 98% α - Al_2O_3 (hexagonal phase). The $MoSi_2$ powder, obtained from Exotherm Corp., Camden, NJ had an average particle size of 45 μm and consisted of α - $MoSi_2$ (tetragonal phase) and a trace of Mo_5Si_3 .

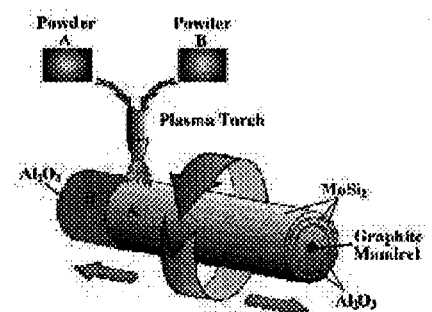


Fig. 1 Schematic representation of the plasma spraying arrangement used to fabricate $Al_2O_3/MoSi_2$ laminated composites [20].

The Al₂O₃ and MoSi₂ powders were sprayed on a graphite mandrel 12.7 mm in diameter. Three different composite microstructures were fabricated while maintaining a constant volume fraction of approximately 50% Al₂O₃ and 50% MoSi₂ by volume. The layer thickness of the composites were varied in order to investigate the influence of layer thickness in the failure mechanisms. The inner layer of each composite consisted of Al₂O₃, while the outer layer consisted of MoSi₂.

Quenching experiments were conducted on bend bar samples (4 mm x 3 mm x 45 mm) machined from the individual spray formed tubes. The samples were held in the furnace at 642°C and at 936°C for approximately 20 minutes and then immersed quickly into a water bath and finally tested for their strength by four-point bending. The tests were performed on an Instron Model 1331 with a crosshead speed of 0.127 mm/min.

Individual tests to determine the material properties that satisfy the R' and R''' relationships were conducted. Bend bar samples were used for four-point bend strength and chevron-notch fracture toughness experiments. An impulse excitation technique (GrindoSonic Model MK5 system) was used to determine the Young's modulus. The coefficients of thermal expansion (CTE) were determined with an Orton dilatometer Model 1000D. The samples were tested between ambient temperature and 1000°C in an argon atmosphere at a rate of 10°C/min. Thermal diffusivity measurements, performed at Thermophysics Inc., Blacksburg, VA, were done on cylindrical samples (1.5-3 mm thickness and 12.7 mm diameter) between ambient temperature and 1000°C in a controlled atmosphere by a laser flash diffusivity method. Thermal conductivity values were then calculated knowing the thermal diffusivity (α), density (ρ), and specific heat (C_p).

Table 1. Processing parameters used for plasma spraying Al₂O₃/MoSi₂ composites.

| Parameter | Value |
|----------------|-------------|
| Current | 850 A |
| Voltage | 25 V |
| Plasma gas | 40-Ar *sclm |
| Powder gas | 40-Ar *sclm |
| Spray distance | 9 cm |
| Hopper speed | 1 rpm |

*sclm: standard cubic liters per minute

3. RESULTS AND DISCUSSION

3.1 Plasma Sprayed Microstructures

The designation and general information for each of the laminated composite configurations are given in Table 2. X-ray diffraction identified both equilibrium and metastable phases. The Al₂O₃ consisted of two distinct phases; metastable γ -Al₂O₃ (major phase) and the equilibrium α -Al₂O₃ phase. The sprayed MoSi₂ resulted in three different phases; equilibrium α -MoSi₂ (major phase), metastable β -MoSi₂, and small trace of Mo₅Si₃. SEM micrographs, of the three laminate composites, showed the discrete layers of each composite in addition to the rough and irregular interfaces, Figure 2.

Table 2. Characteristics of as-received plasma sprayed materials

| Material | Sample ID | Porosity* | Number of Layers | Layer Thickness** (μm) | |
|--------------------------------|-----------|-----------|------------------|-------------------------------------|-------------------|
| | | | | Al ₂ O ₃ | MoSi ₂ |
| Thin layered composite | MSA1 | 19.6 | 112 | 61 \pm 20 | 49 \pm 20 |
| Intermediate layered composite | MSA2 | 14.8 | 26 | 184 \pm 50 | 226 \pm 80 |
| Thick layered composite | MSA3 | 19.5 | 10 | 690 \pm 100 | 670 \pm 100 |

*Total porosity using gas pynometry and Archimedes method.

**Determined by the line count (L_L) technique.

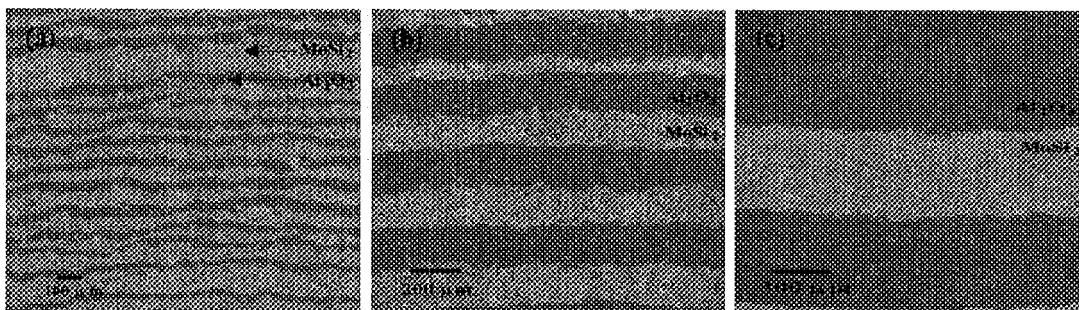


Fig. 2 SEM microstructure images of the $\text{Al}_2\text{O}_3/\text{MoSi}_2$ laminated composites. (a) The thin layered composite MSA1, (b) intermediate layered thickness composite MSA2, and (c) thick layered composite MSA3. Al_2O_3 (dark phase) MoSi_2 (light phase).

3.3 Quenching Experiments

The change in strength decreased gradually rather than showing an abrupt change after quenching samples from 642°C and 936°C to room temperature, Figure 3. Only the thick layered composite revealed a larger drop in the strength as compared to the other composites. Tests were not conducted between $400\text{-}600^\circ\text{C}$ in order to avoid the pesting reaction which occurs in MoSi_2 . No catastrophic failure occurred, instead all the samples remained intact after the thermal shock. Microscopic visible cracks were observed primarily in the Al_2O_3 layers of the thick layered composite samples. Upon further investigation by SEM analysis, all three samples showed the presence of cracks continuing in the MoSi_2 layer with minimal deflection at the interface, indicating a strong bond at the interface. The cracks typically propagate perpendicular to the interface in the MoSi_2 layers, while in the Al_2O_3 layers, the cracks also propagate perpendicular to the interface with some deflection occurring within the layers. Cracks running parallel to the interface were also observed. The deflection and crack branching occurs due to the compressive residual stresses present in the Al_2O_3 layers caused by the thermal expansion mismatch between the two materials [7]. Cylindrical ring samples were sectioned from the spray formed tubes for additional quenching experiments in order to observe the cracking behavior in the cylindrical samples. Samples were quenched in water at a ΔT of 700, 800, 900, and 1000°C . The crack behavior observed in the cylindrical samples were similar to the cracks in the bend bars. Figure 4 shows the crack patterns seen in the thick

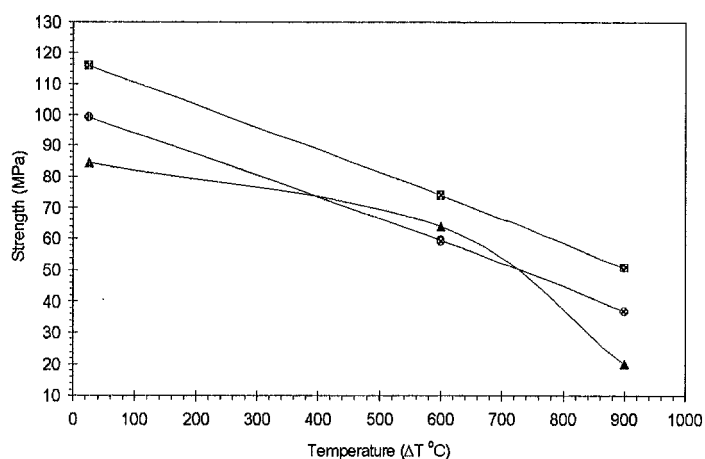


Fig. 3 Drop in strength as a function of the temperature change (ΔT) for the $\text{Al}_2\text{O}_3/\text{MoSi}_2$ laminated composites. ■ MSA1 composite, ● MSA2 composite, and ▲ MSA3 composite.

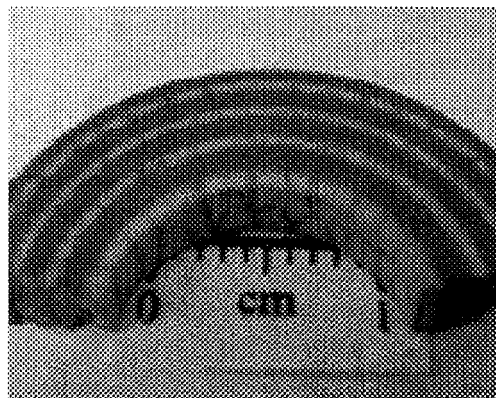


Fig. 4 Cracking behavior of the thick layered composite after thermal shock testing (ΔT of 900°C).

layered composite sample tested with a ΔT of 900°C. An additional set of cylindrical samples were quenched five times from 900°C to room temperature water to observe the cracking behavior. Upon the second thermal shock of the thick layered composite, a large crack was produced which ran radially through the thickness. The thin layered composite showed a surprisingly graceful failure mode where cracking occurred along individual layers of the composite, resulting in the separation of ring sections from the material. The material surprisingly did not catastrophically fail (Figure 5a). No visible damage was observed for the intermediate layered composite, which was visibly intact after all five thermal shock treatments (Figure 5b). After the third thermal shock, the thin layered composite continued to delaminate while the thick layered composite catastrophically failed by having a section fracture off. Figure 5 shows representative cracking behavior of the thin layered and thick layered composites during various stages of the thermal shocks. No changes were observed for the thin and thick layered composites after the third thermal shock treatment.

3.3 Thermal Shock Resistance R' and R''''

The material properties determined in this investigation are given in Table 3. These values are substantially lower when compared to conventionally processed samples due to the porosity. The Poisson's ratios were not determined due to sample constraints; rather reference values [21,22] for monolithic Al_2O_3 and $MoSi_2$ were used. Using the values in Table 3, R' and R'''' were determined for each of the composites.

Table 3. Selected material properties of plasma sprayed $Al_2O_3/MoSi_2$ structures.

| Sample ID | σ_f (MPa) | K_{IC} (MPa \sqrt{m}) | E (GPa) | CTE* ($\times 10^{-6} K^{-1}$) | k ** (W/ m K) | R' (W/m) | R'''' (μm) |
|-----------|------------------|----------------------------|---------|----------------------------------|---------------|------------|---------------------|
| MSA1 | 116 | 3.3 | 129 | 8.14 | 5.30 | 474 | 1000 |
| MSA2 | 99 | 2.9 | 102 | 7.88 | 3.22 | 321 | 1061 |
| MSA3 | 84 | 2.1 | 86 | 8.14 | 2.93 | 284 | 773 |

* value average from RT to 1000°C

**value taken from the RT reading

From the values in Table 3, the thin layered composite was shown to have the best fracture initiation resistance (R') value at 474 W/m. The intermediate layered composite showed the best crack propagation resistance (R'''') value at 1061 μm and correlated with the quenching results which showed the sample intact after the thermal shock treatments.

4. CONCLUSIONS

Thermal shock evaluations by either quenching experiments or numerical relationships are a few methods of determining the thermal shock resistance of specific materials. Nevertheless, the evaluation of two distinct methods can provide different points of view in understanding the thermal shock behavior to a common conclusion. Applications where the thermal protection is vital, such as

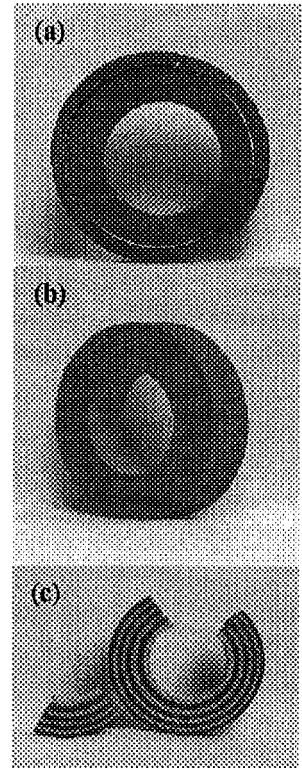


Fig. 5 $Al_2O_3/MoSi_2$ laminated composites showing their thermal shock behavior after numerous quenches. (a) MSA1 composite after 3 shocks, (b) MSA2 composite after 5 shocks, and (c) MSA3 composite after 3 shocks.

in refractory materials, the spalling or removal of material is unacceptable thus the manner in which cracks propagate becomes a determining factor.

Three different plasma sprayed $\text{Al}_2\text{O}_3/\text{MoSi}_2$ layered thickness laminated composites were fabricated in a tube geometry. The layer thicknesses ranged from 49-690 μm . Microstructure characterization identified equilibrium and metastable phases present and showed the rough and irregular interfaces.

Quenching experiments on $\text{Al}_2\text{O}_3/\text{MoSi}_2$ laminate bend bars showed a gradual decrease in the strength rather than a drastic drop in the range from room temperature to 1000°C.

Cylindrical samples quenched in water from the range of 600-1000°C down to room temperature remained intact. The cracking behavior showed cracks running perpendicular to the interface in the MoSi_2 layers and propagating into the Al_2O_3 layers where crack branching and deflection occurred due to the compressive and tensile stresses associated with the thermal expansion mismatch.

Additional cylindrical samples were thermal shock treated five times from a ΔT of 900°C. The thick layered composite catastrophically failed after the third thermal shock treatment. The thin layer composite began to fail in a graceful manner by the delamination of ring sections. The intermediate layered composite showed no visible damage and remained intact after the five thermal shock treatments. SEM analysis revealed microcracks throughout the three composite structures.

The strength, fracture toughness, Young's modulus, thermal expansion, and thermal conductivity were determined for the three laminated composites and used in evaluating the thermal shock resistance by R' and R'''' relationships. The thin layered composite was shown to have the best fracture initiation resistance (R') value at 474 W/m, while the intermediate layered composite had the best crack propagation resistance (R'''') value at 1061 μm .

ACKNOWLEDGEMENTS

The authors would like to acknowledge the DOE/OIT/AIM/-Glass Industry, Materials Science Technology Division, and the University of Alabama at Birmingham for supporting various aspects of this research done at Los Alamos National Laboratory. They would also like to acknowledge many other people at Los Alamos National Laboratory who have contributed to the research activity there.

REFERENCES

- [1] W. D. Kingery, "Factors Affecting Thermal Stress Resistance of Ceramic Materials," *J. Amer. Cer. Soc.*, **38** [1] 3-15 (1955).
- [2] B. A. Boley and J. H. Weiner, *Theory of Thermal Stresses*. John Wiley & Sons, Inc., New York, 1960.
- [3] D. P. H. Hasselman, "Unified Theory of Thermal Shock Fracture Initiation and Crack Propagation in Brittle Ceramics," *J. Amer. Cer. Soc.*, **52** [11] 600-04 (1969).
- [4] D. P. H. Hasselman, "Elastic Energy at Fracture and Surface Energy as Design Criteria for Thermal Shock," *J. Amer. Cer. Soc.*, **46** [11] 535-40 (1963).
- [5] D. P. H. Hasselman, "On the Nature of Crack Propagation During Thermal Shock of Brittle Ceramics," pp. 485-94 in *Fracture Mechanics of Ceramics*, Vol. 11. Edited by R. C. Bradt, D. P. H. Hasselman, D. Munz, M. Sakai, and V. Y. Shevchenko. Plenum Press, New York, 1996.
- [6] Z. Jin and Y. Mai, "Effects of Damage on Thermal Shock Strength Behavior of Ceramics," *J. Amer. Cer. Soc.*, **78** [7] 1873-81 (1995).
- [7] Z. Chen and J. J. Mecholsky Jr., "Damage-tolerant Laminated Composites in Thermal Shock," *J. Mater. Sci.*, **28** 6365-70 (1993).

- [8] H. A. Bahr, G. Fischer, and H. J. Weiss, "Thermal-shock Crack Patterns Explained by Single and Multiple Crack Propagation," *J. Mater. Sci.*, **21** 2716-20 (1986).
- [9] M. V. Swain, "R-Curve Behavior and Thermal Shock Resistance of Ceramics," *J. Amer. Cer. Soc.*, **73** [3] 621-28 (1990).
- [10] M. V. Swain, "Thermal Shock of Brittle Materials," pp. 473-84 in *Fracture Mechanics of Ceramics*, Vol. 11. Edited by R. C. Bradt, D. P. H. Hasselman, D. Munz, M. Sakai, and V. Y. Shevchenko. Plenum Press, New York, 1996.
- [11] T. K. Gupta, "Strength Degradation and Crack Propagation in Thermally Shocked Al_2O_3 ," *J. Amer. Cer. Soc.*, **55** [5] 249-53 (1972).
- [12] K. Matsushita, S. Kuratani, T. Okamoto, and M. Shimada, "Young's Modulus and Internal Friction in Alumina Subjected to Thermal Shock," *J. Mater. Sci. Lett.*, **3** 345-48 (1984).
- [13] B. S. Hahn and H. L. Lee, "Effect of Environmental Factors on Thermal Shock Behavior of Polycrystalline Alumina Ceramics," *J. Mater. Sci.*, **34** 3623-30 (1999).
- [14] M. Saadaoui and G. Fantozzi, "Crack Growth Resistance Under Thermal Shock Loading of Alumina," *Mater. Sci. Eng.*, **A247** 142-51 (1998).
- [15] J. B. Wachtman, "Linear Elastic Fracture Mechanics"; pp. 46-63 in *Mechanical Properties of Ceramics*, John Wiley & Sons, New York, US, 1996.
- [16] E. H. Lutx, "Plasma Ceramics," *Powder Metall. Int.*, **25** [3] 131-37 (1993).
- [17] H. Herman, "Plasma-sprayed Coatings," *Scientific Amer.*, [9] 112-17 (1988).
- [18] R. McPherson, "A Review of Microstructure and Properties of Plasma Sprayed Ceramic Coatings," *Surface Coating Tech.*, **39/40** 173-81 (1989).
- [19] R.B. Heimann, in *Plasma-Spray Coating*. Edited by P. Gregory and U. Anton. VCH Publishers, New York, US, 1996
- [20] A. H. Bartlett, R. G. Castro, D. P. Butt, H. Kung, J. J. Petrovic, and Z. Zurecki, "Plasma Sprayed $\text{MoSi}_2/\text{Al}_2\text{O}_3$ Laminate Composite Tubes as Lances in Pyrometallurgical Operations," *Industrial Heating*, **63** [1] 33-6 (1996).
- [21] A. Misra, F. Chu, and T.E. Mitchell, "Elastic Properties of Intermetallic Compound ReSi_2 ," *Scripta Mater.*, **38** [6] 917-21 (1998).
- [22] K.K. Chawla, "Ceramic Matrix Materials"; pp. 95-100 in *Composite Materials: Science and Engineering*, 2nd Ed. Springer-Verlag, New York, US, 1998.